ACS OMEGA

Open Access



http://pubs.acs.org/journal/acsodf

Article

# Colorimetric and Reverse Fluorescence Dual-Signal Readout Immunochromatographic Assay for the Sensitive Determination of Sibutramine

Yun Gui, Yun Zhao, Pengyan Liu, Yulong Wang, Xinxin Mao, Chifang Peng, Bruce D. Hammock, and Cunzheng Zhang*

Cite This: *ACS Omega* 2024, 9, 7075−7084

Read Online

ACCESS | Metrics & More | Article Recommendations | Supporting Information

**ABSTRACT:** Later flow immunochromatographic assay has been widely used in clinical, environmental, and other diagnostic applications owing to its high sensitivity and throughput. However, most immunoassays operate in the "turn-off" mode for detecting targets of low molecular weight. The signal intensity decreases as the analyte concentration increases, which poses a challenge for achieving ultrasensitive detection at low concentrations and is counterintuitive to new users. In this work, a fluorometric immunochromatographic assay (FICA) is developed to simultaneously read "turn-on" fluorescent and "turn-off" colorimetric signals, where ZnCdSe/ZnS quantum dots act as fluorescence donors and gold nanoparticles (AuNPs) act as quenchers. The fluorescent signal (excitation/emission wavelengths of 365/525 nm) is positively correlated with analytes' concentration. Taking sibutramine (SBT) as the analysis target, the visual limit of detection for SBT reached 3.9 ng/mL, and the limit of Quantitation was 5.0 ng/mg in spiked samples. The developed FICA achieves a high sensitivity in SBT detection, which is much lower than that of the colloidal gold-based immunochromatographic assay. This dual-function detection mode has great potential to be used as a rapid on-site semiquantitative method, providing an alternative mode for the determination of low levels of target analytes.

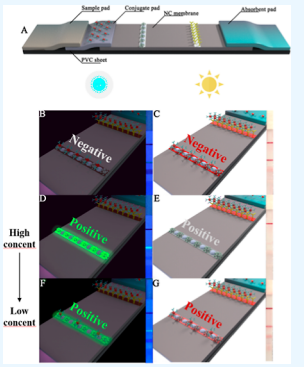


## INTRODUCTION

Sibutramine (SBT) was approved as an antiobesity drug by the U.S. Food and Drug Administration (FDA) in 1997 and was also regarded as an effective drug for treating obesity in European countries.[1,2] As a serotonin-norepinephrine reuptake inhibitor, its weight loss mechanism is achieved by inhibiting and activating the satiety center and increasing energy expenditure.[3,4] However, further studies have shown that ingestion of SBT increases cardiovascular and nonfatal stroke risk, a dangerous side effect that has banned its use in many countries.[5,6] Therefore, in 2010, the FDA, the European Commission, and the Ministry of Health of the People's Republic of China banned SBT and recommended that its production, sale, and use be stopped.[5,7] However, due to its tremendous weight loss effects, some weight loss supplements still illegally add SBT to increase weight loss. SBT has been detected in many so-called antiobesity and natural weight-loss products in the market. This adulteration of products can present a real risk to consumers and damage the credibility of legitimate products. For both customers and regulators, a rapid, sensitive, affordable, and self-service-accessible approach is needed.

At present, instrumental-based approaches for the detection of SBT have undergone substantial development and have achieved extensive utilization; for example, electrospray ionization mass spectrometry (ESI-MS),[8] high-performance liquid chromatography (HPLC),[9] gas chromatography (GC),[10] Fourier transform infrared spectroscopy (FTIR),[11] and other instrumental methods have been developed. These instrumental analytical methods generally possess high capacity for trace component detection and excellent accuracy, but superior sensitivity comes with a high equipment and maintenance cost, as well as the need for highly trained professionals. In recent years, some innovative analytical approaches offering good sensitivity and convenience were proposed, such as surface-enhanced Raman scattering senor (SERS)[12] and glassy carbon electrode (GCE),[13,14] but they remain equipment intensive. These methods are inconvenient for testing personnel to screen suspicious samples rapidly under field conditions.

Lateral flow immunochromatographic analysis (LFIA) is a rapid, low-cost, and convenient detection method, which has excellent performance in food safety detection and on-site diagnosis.[15,16] Currently, LFIA has been used for the

Received: November 13, 2023
Revised: December 24, 2023
Accepted: January 15, 2024
Published: February 2, 2024





https://doi.org/10.1021/acsomega.3c09050
*ACS Omega* 2024, 9, 7075−7084

qualitative and semiquantitative detection of SBT based on the antigen−antibody biochemical interaction.[17,18] In these systems, a signal reporter of gold nanoparticles offers excellent stability and optical properties while fluorescent quantum dots (QDs) offer high fluorescence quantum yield and tunable emission wavelength. Yet background signal intensity limits ultrasensitive detection.[19,20] For micromolecular analyte detection, current LFIA presents a competitive mode called "turn-off", and there is a negative correlation between the measured signal intensity and target concentration.[21,22] The limit of detection (LOD) of LFIA in "turn-off" mode is defined as the corresponding concentration of analytes causing the apparent signal to completely disappear.[23] For the "turn-off" mode, the intensity of the visualized signal decreases rather than disappears when low concentrations of analyte are present, making it difficult to determine whether a low concentration of analyte is present.

Gold nanoparticles possess large extinction coefficients and wide characteristic absorption peaks in the visible range that overlap with the emission spectrum of fluorescent materials.[24] Quantum dots (QDs) have outstanding properties such as high quantum yield, tunable photoluminescence emission, high molar extinction coefficients, narrow and symmetric fluorescence spectra, large Stokes shift, high photochemical stability, chemical stability, and other advantages.[25,26] By exploiting the phenomenon of quenching in the presence of spectrally overlapping fluorescence signals from these two materials, they were shown to be excellent quenchers and donors for the preparation of "turn-on" type fluorescence immunochromatographic assays (FICAs). Sheng et al.[27] developed a fluorometric lateral flow immunoassay in "turn-on" mode to detect tetracycline based on QDs fluorescence quenching by gold nanoparticles. Chen et al.[28] constructed a high fluorescence quenching probe-based reverse fluorescence enhancement lateral flow test strip (rLFTS) to realize the detection of the relevant nucleic acid of Parkinson disease.

In this study, a FICA was constructed based on a combination of QDs as fluorescent signal source and gold nanoparticle as fluorescence quencher. As the SBT content increases, the fluorescence signal gradually increases, and the colorimetric signal gradually weakens. It not only retains the "turn-off" mode of LFIA but also proposes a "turn-on"mode for fluorescence signal interpretation through ultraviolet light (UV) to achieve visual detection of low-concentration SBT.

## MATERIALS AND METHODS

**Materials and Instruments.** Sibutramine hydrochloride, ovalbumin (OVA), 1-ethyl-3-[3-(dimethylamino) propyl] carbodiimide (EDC), and chloroauric acid ($HAuCl_4$) were purchased from Sigma-Aldrich Chemical Co, Ltd. (St. Louis, MO, USA). Carboxyl functional ZnCdSe/ZnS quantum dots (QDs) (emission maximum at 525 nm) were obtained from Jiayuan Quantum Dots Co, Ltd. (Wuhan, China). Trisodium citrate dihydrate (SC) was purchased from Sinopharm Chemical Reagent Co, Ltd. (Shanghai, China). Anti-SBT monoclonal antibody (mAb) and SBT coating antigen (SBT-OVA) were produced in our laboratory. Goat antimouse antibody was obtained from Solarbio Biotechnology Co, Ltd. (Beijing, China). Enzyme-linked immunosorbent assay (ELISA) PLATE, poly(vinyl chloride) (PVC) sheet, absorbent pad, conjugate pad, sample pad, and nitrocellulose (NC) membrane were purchased from Thermo Fisher Scientific (Waltham, MA, USA). Automatic guillotine cutter (CM4000) and dispensing platform (XYZ3050) were purchased from BioDot Co, Ltd. (Irvine, CA, USA). The immunochromatographic assay signal reader was obtained from Helmence Instrument Co, Ltd. (Suzhou, China). A portable UV lamp was purchased from LICHEN Scientific Co, Ltd. (Qingdao, China).

**Preparation of QDs-OVA.** The conjugation of OVA and QDs was performed by previously described methods with slight modifications as described below.[29,30] In brief, 100 μL of carboxy-surface QDs (8 μmol, dissolved in 50 mmol borate buffer) were diluted with 10 mmol sodium borate (pH 8.6) to a final concentration of 1 μmol. The pH of the diluted QDs solution was adjusted to 5.5 using a citric acid−sodium citrate buffer (0.1 M). Then, 15 μL of EDC solution (10 mg/mL) was added to the above solution and stirred for 4 h in the dark. Subsequently, 1.35 mg of OVA was added to continue the reaction for 12 h. Finally, the resulting mixture was centrifuged for 15 min (13,000 rpm, 4 °C), the supernatant was discarded, and the pellet was redissolved in 100 μL of PB (0.01 M, pH 7.4) and stored at 4 °C.

**Preparation of AuNPs and Au-mAb Probes.** The AuNPs were synthesized on the basis of previous work,[31] and the anti-SBT mAb was obtained previously.[32] 0.1 M $K_2CO_3$ was added to the prepared AuNPs solution (1 mL, 0.18 nmol/L) to adjust pH to 7, 8, 9, 10, 11, and 12, then 2.5, 5, 10, and 20 μg of anti-SBT mAb was added. Afterward, the reaction mixture was incubated for 1 h at room temperature. To block the uncoupled surface of AuNPs, 10 μL volumes of 20% BSA solution and 20% PEG-20,000 were added and incubated for 30 min to avoid nonspecific adsorption. Then, the solution was centrifuged for 30 min (10,000 rpm, 4 °C). Finally, the precipitate was resuspended in 1 mL of ultrapure water, and the Au-mAb probe was obtained.

**Fabrication of FICA Strip.** The FICA was developed by referring to the work reported and processed as following.[27] A mixture of 50 μL of QDs-OVA (450 nmol/L) and 50 μL of SBT-OVA (0.25 mg/mL) were sprayed on the reaction membrane at a dose of 0.6 μL/cm as the T line. Analogously, goat antimouse antibody (1 mg/mL) was immobilized on NC membrane as C line with a 0.6 μL/cm dosage. After 4 h of drying at 37 °C, all of the parts mentioned above were cut into 3 mm strips, stored at room temperature, and kept under desiccation.

**Optimization.** To optimize the pH of the synthesis of the Au-mAb probe, the pH of the AuNP solutions were adjusted to 7, 8, 9, 10, 11, and 12. To optimize the amount of immobilized antibody, 2.5, 5, 7.5, and 10 μg of anti-SBT mAb was added dropwise to 1 mL of AuNPs solution at final concentrations of 2.5, 5, 7.5, and 10 μg/mL, respectively. To optimize the SBT-OVA concentration, the T line was sprayed with SBT-OVA at concentrations of 0.1, 0.25, 0.5, 0.75, and 1.0 mg/mL with a spraying speed of 0.6 μL/cm.

In the above-mentioned experiments, the addition of PBS (0.01 M) buffer containing 0 and 100 ng/mL SBT was used to optimize the key parameters. The pixels per inch (ΔPPI) of colorimetric signal on the T line was monitored as the indicator of optimization. ΔPPI gives the difference value of the T line signal between negative (0.01 M PBS) and positive (100 ng/mL SBT in 0.01 M PBS) controls ($\Delta PPI = PPI_{negative} - PPI_{positive}$). On the basis of the optimized conditions, the optimal quenching efficiency between donors and receptors is established. Final concentrations of 300, 450, and 600 nmol/L QDs-OVA mixed with SBT-OVA were sprayed on the T line,


https://doi.org/10.1021/acsomega.3c09050
ACS Omega 2024, 9, 7075−7084

Scheme 1. Schematic Illustration of the FICA[a]

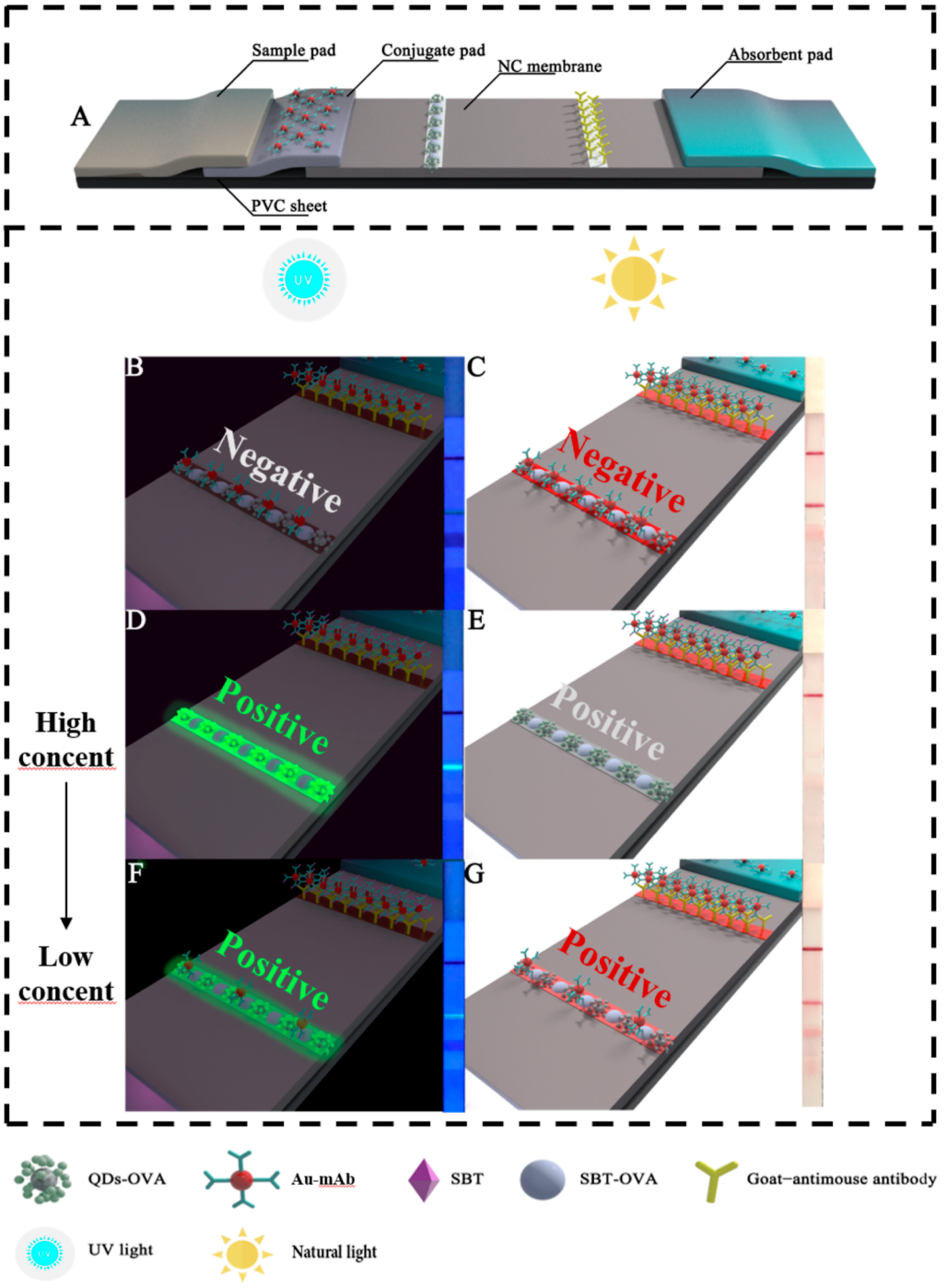


[a](A) construction of FICA strip, negative sample detection under (B) UV light and (C) natural light, positive sample detection under (D, F) UV light and (E, G) natural light.

and 0, 0.25, 0.5, 0.75, 1.0, and 2.0 $\mu$L of Au-mAb was dried on conjugation pad. Then 0, 0.98, 1.95, 3.90, 7.81, 15.63, 31.25, 62.5, 125, and 250 ng/mg of SBT-containing PBS (0.01 M, pH 7.4) buffer was added for detection according to each of the above-mentioned protocols. The best correlation was found, responding to the lowest concentration of SBT. All experiments were performed in triplicate.

**Method Validation.** Two types of dietary fiber soft capsules and weight loss supplement tablets in e-commerce stores were randomly purchased as samples and were confirmed by free LC−MS/MS. For analysis, accurately weighed 895.3 mg of ground and homogenized capsule contents or tablets were spiked with SBT standards to final concentrations of 2, 5, 100, and 250 ng/mg. The samples were dissolved in 30 mL of methanol, vortexed for 10 min, subjected to ultrasonic extraction for 15 min (at a water bath temperature of 40 °C), and then centrifuged for 5 min (4000 rpm, 25 °C). The supernatant was collected and dried under a $N_2$ stream, then redissolved in 50 mL of PBS containing 5% methanol, vortexed for 30 s, and filtered



https://doi.org/10.1021/acsomega.3c09050
ACS Omega 2024, 9, 7075−7084

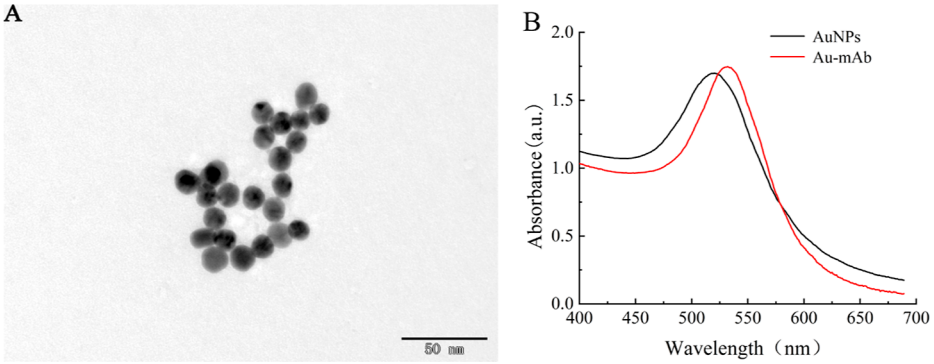


**Figure 1.** Characterization of AuNPs and Au-mAb. (A) TEM images of AuNPs. (B) UV−vis absorption spectra of AuNPs and Au-mAb.

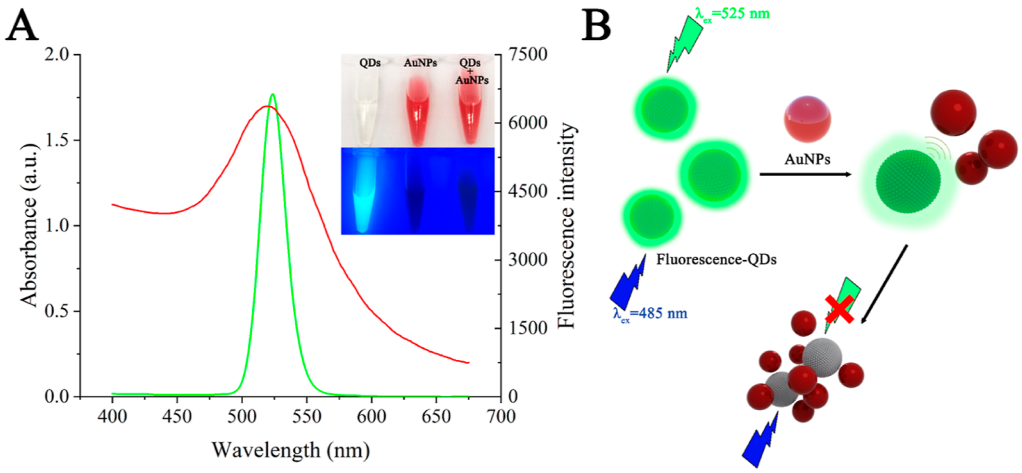


**Figure 2.** (A) UV−vis absorption spectrum of AuNPs and fluorescence spectrum of QDs. (B) Process representation of the fluorescence quenching mechanism by AuNPs.

through a 0.22 $\mu$m Teflon membrane. The extracts were further diluted 16-fold in PBS containing 5% methanol to suppress the interference of matrix and then ready for the analysis of FITC and LC−MS/MS.

**Performance of FICA.** As illustrated in Scheme 1A, QDs were labeled on the OVA as fluorescent emitters, and the conjugate of QDs-OVA was sprayed evenly on the T line. The mAb-labeled AuNPs as probes and quenchers were precoated on the conjugate pad and kept dry. In the absence of SBT, Au-mAb and SBT-OVA formed a sandwich structure, resulting in a close adjacency of AuNPs and QDs. Then, concomitant arresting fluorescence quenching occurred on the T line (Scheme 1B), and no fluorescence signal would be observed under UV light. Meanwhile, AuNPs aggregation induced color emergence, which allowed naked eye readout (Scheme 1C). In contrast, when the sample contained a high concentration of SBT, the Au-mAb complex was unable to bind with SBT-OVA on the T line, and the fluorescence was restored; thus, a strong green fluorescence signal was observed (Scheme 1D), but no colorimetric signal was detected (Scheme 1E). However, a relatively low target concentration might cause a visible weak colorimetric signal to appear (Scheme 1G), resulting in a false-negative judgment by the naked eye. Under this circumstances, a green fluorescence signal still appeared in UV light (Scheme 1F), which ensures the identification of low concentrations of SBT. Thus, the developed FICA with simultaneous "turn-on" and "turn-off" modes achieved a dual-signal readout, supporting ultrasensitive semiquantitative and rapid large-scale screening.

## RESULTS AND DISCUSSION

**Characterization of AuNPs and Au-mAb.** The morphology and size of AuNPs are illustrated via the transmission electron microscopy (TEM) image in Figure 1A. It revealed that the size of AuNPs was 20 ± 0.7 nm with a uniform dispersion. In the UV−vis absorption spectrum (Figure 1B), the maximum absorption peak of Au NPs was 519 nm, the narrow peak shape could be observed, indicating a stable state of dispersion, and the small red shift was attributed to the coupling of antibody with AuNPs.

**Reaction Mechanism Exploration.** AuNPs were highly efficient fluorescence quenchers of molecular excitation energy (up to 99.8%) over a long distance (about 40 nm) because of their extremely strong absorption.[33,34] ZnCdSe/ZnS QDs were chosen as the donors to construct luminophore-AuNPs composites due to their slower diffusion of excitons to dissociative defects, leading to a relatively brighter emission.[35] Figure 2A showed the absorption spectrum of the AuNPs (surface plasmon maximum at 519 nm), which had a large degree of overlap with the emission spectrum of the QDs (emission maximum at 525 nm). Figure 2B illustrates that the fluorescence was gradually extinguished with the narrowing distance between QDs and AuNPs. Fluorescence quenching modes include the "on−off" method, which can be summarized as follows: (a) by reducing the light emission



https://doi.org/10.1021/acsomega.3c09050
ACS Omega 2024, 9, 7075−7084

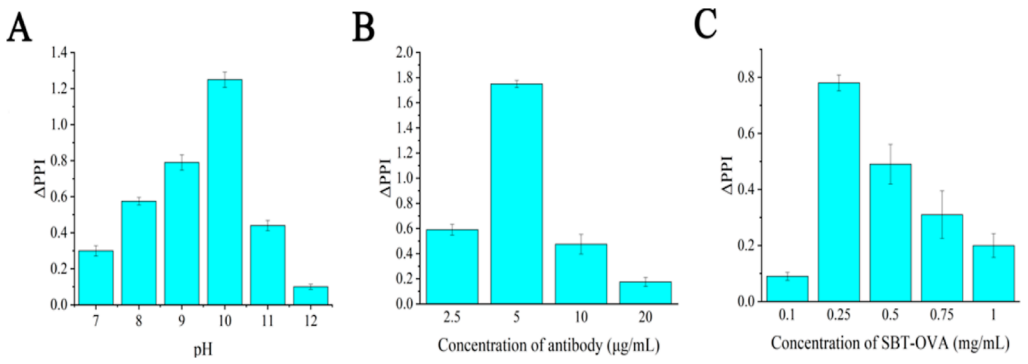


**Figure 3.** Optimization of key parameters. ΔPPI of the T line at different (A) pH values, (B) antibody concentrations, and (C) SBT-OVA concentration.

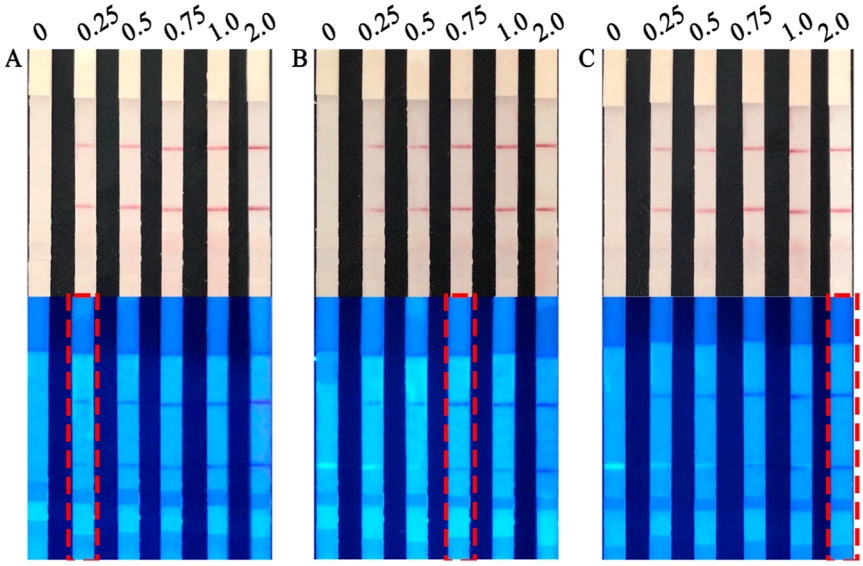


**Figure 4.** Fluorescence quenching relationship between 0, 0.25, 0.5, 0.75, 1.0, and 2.0 μL of Au-mAb and (A) 300, (B) 450, and (C) 600 nmol/L of QDs-OVA.

intensity of fluorescent nanoprobes. (b) "On-off-on" approach by breaking the bond between the fluorescent nanoprobe and the analyte. (c) "Postfunctionalization" method, chemically modifying the surface of prepared fluorescent nanoparticles to introduce specific receptor molecules or other molecular functional groups so that the probe has specific biological recognition or chemical response characteristics.[36] Obviously, FICA in this study belongs to the third mode. In this detection process, the vast majority of quenching mechanisms relies on fluorescence resonance energy transfer (FRET),[30,37] inner filter effect (IFE),[37,38] and nanometal surface energy transfer (NEST).[38] In this study, the emission spectrum of the QDs overlapped with the UV absorption spectrum of the AuNPs, which met the requirements of fluorescent material (donor) and quencher (acceptor) in FRET and IFE. The prerequisite for FRET is that the distance between fluorescence donor and acceptor needs to be less than 10 nm.[39] The mixture of QDs-OVA (donor) and SBT-OVA was sprayed on the T line and the proximity between AuNPs (acceptor) and QDs-OVA relied on the specific binding of antigen and antibody, but it is hard to ensure the ideal distance between QDs and AuNP to generate FRET.[27] IFE becomes the crucial factor for fluorescence quenching. IFE needs to meet the requirements of only spectral overlap for the quenching phenomenon to occur. It does not have strict requirements on the distance between the donor and the acceptor, which becomes a key factor leading to fluorescence quenching in this study.[36] Some research suggested that the primary cause of fluorescence quenching in LFIA was attributed to the IFE and the self-absorption of fluorescence.[40,41] Besides, Nebu et al.[38] and Yao et al.[34] considered that the system followed NEST, in which interaction between donor and acceptor was generated through an electromagnetic field by the fluorescent material dipole and the conduction band charge of AuNPs. Here, either the IFE or NEST could lead to fluorescence quenching. Therefore, the developed FICA with a dual-signal readout is anticipated to offer enhanced sensitivity compared to that of the single-signal-based AuNPs IFCA, serving as an on-site rapid diagnostic strategy for the accurate detection of trace analytes.

**Optimization.** Before matching the QD fluorescence emitter with the amount of AuNPs quencher, we optimized key parameters of the FICA assay to achieve the best detection performance. In order to improve the detection sensitivity of SBT, we employed ΔPPI as our analytical metric for result assessment. The magnitude of fluorescent restoration is directly related to the amount of Au-mAb combined on the T line, which is positively correlated with the amount of


https://doi.org/10.1021/acsomega.3c09050
ACS Omega 2024, 9, 7075−7084

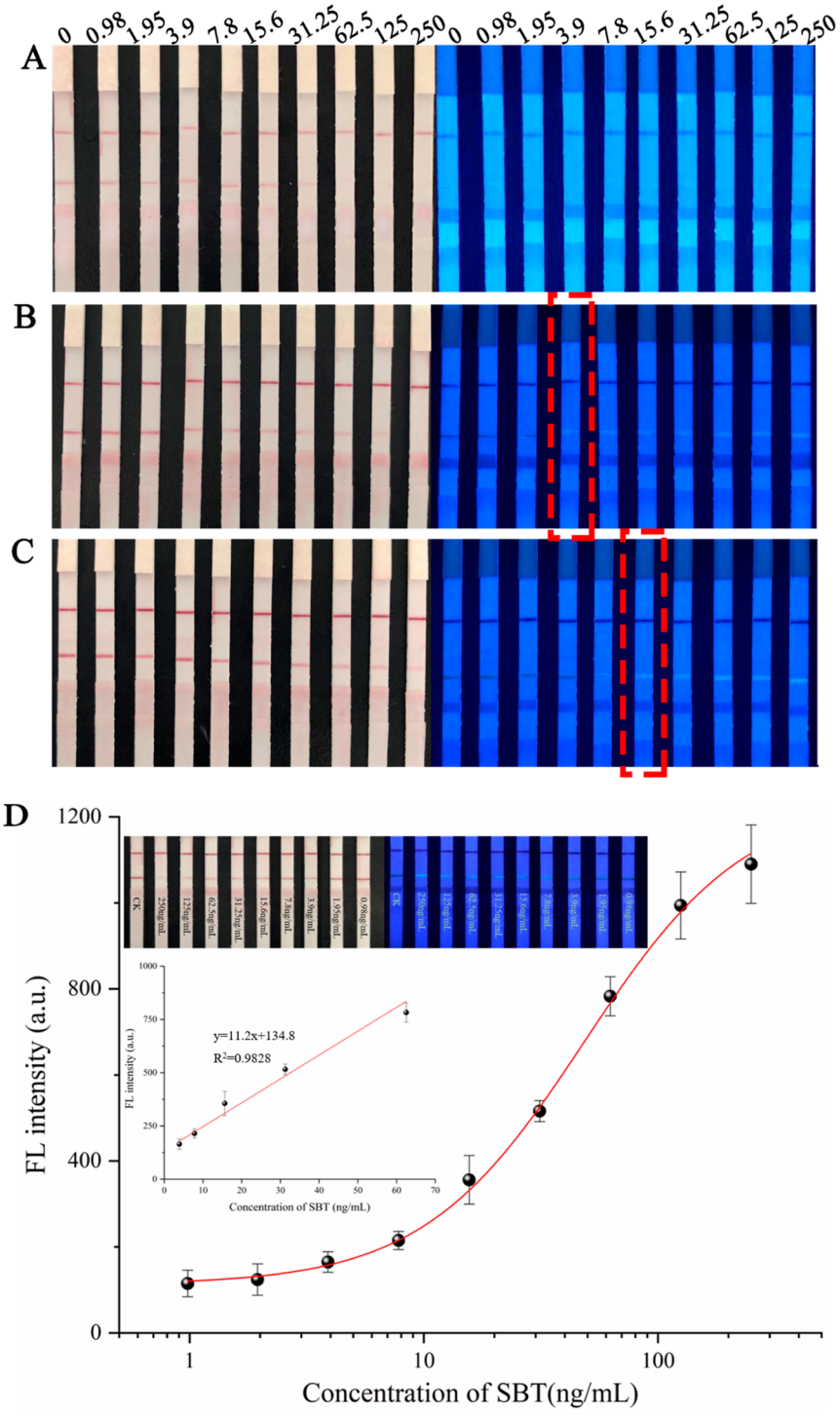


**Figure 5.** Detection of SBT in PBS at 0, 0.98, 1.95, 3.9, 7.8, 15.6, 31.25, 62.5, 125, and 250 ng/mL for (A) 0.25 $\mu$L of Au-mAb and 300 nmol/L QDs-OVA, (B) 0.75 $\mu$L of Au-mAb and 450 nmol/L QDs-OVA, (C) 2 $\mu$L of Au-mAb and 600 nmol/L QDs-OVA, and (D) standard curve for quantitative analysis of SBT through changes in T-line fluorescence intensity. The inset shows the linear relationship in the low concentration range and the actual plot.

analytes in the sample. Therefore, the higher the ΔPPI, the higher the detection sensitivity.

Figure 3A shows the effect of the pH on PPI. ΔPPI reached its maximum value at pH = 10 and then decreased with the increase of pH, indicating that pH = 10 was the optimum pH condition for the coupling process. Figure 3B shows the effect of the antibody addition on ΔPPI. ΔPPI peaked when 5 $\mu$g of antibody was added to 1 mL of AuNPs solution for probe coupling. As the amount of antibody added increased from 5 to 20 $\mu$g, ΔPPI decreased due to supersaturation of the antibody adsorbed to the probe on the T-line. Therefore, 5 $\mu$g was selected as the optimal antibody addition amount. Figure 3C shows the effect of SBT-OVA on ΔPPI. As the concentration increased from 0.1 to 1 mg/mL, ΔPPI peaked and gradually decreased. In order to obtain a higher ΔPPI, the optimum



https://doi.org/10.1021/acsomega.3c09050
ACS Omega 2024, 9, 7075−7084

spraying concentration of SBT-OVA on the T line was 0.25 mg/mL (spraying speed 0.6 μL/cm).

**Visual Sensitivity Assessment of the FICA.** The visual limit of detection (vLOD) of FICA in this work was defined as the lowest concentration of SBT at which the colorimetric signal began to decrease under natural light, and at the same time a green fluorescent signal appeared under 385 nm UV light. It was the key to finding an appropriate match between QDs-OVA and Au-mAb to make the FICA sensitively respond to the change of analytes amounts, and the fluorescence could be completely quenched in the negative condition. Under optimized conditions, 0, 0.25, 0.5, 0.75, 1.0, and 2.0 μL volumes of Au-mAb (0.18 nmol/L) probes were dried on the conjugate pad, and optimized SBT-OVA (0.25 mg/mL, spraying speed 0.6 μL/cm) was mixed with final concentrations of 300, 450, and 600 nmol/L QDs-OVA and sprayed on the T line. Through detection of blank samples (PBS), the minimum volume quenching fluorescence was deemed to be the optimal addition of Au-mAb. As shown in Figure 4, 0.25, 0.75, and 2.0 μL of Au-mAb (0.18 nmol/L) were the minimum volumes for 300, 450, and 600 nmol/L QDs-OVA (0.25 mg/mL, spraying speed 0.6 μL/cm) fluorescence quenching, respectively. Then, a series of concentrations of SBT standard solution (0, 0.98, 1.95, 3.9, 7.8, 15.6, 31.25, 62.5, 125, and 250 ng/mL) were detected in the 0.25 μL-300 nmol/L (Figure 4A), 0.75 μL-450 nmol/L (Figure 4B), and 2.0 μL-600 nmol/L schemes (Figure 4C).

The results are shown in Figure 5, and as the concentration of SBT increases, the fluorescence intensity on the T line increases gradually. However, Figure 5A showed that the green fluorescence signal is indecipherable to recognize for 300 nmol/L QDs-OVA (0.25 mg/mL, spraying speed 0.6 μL/cm) with related 0.25 μL of Au-mAb (0.18 nmol/L). As shown in Figure 5B, when the concentration of SBT reached 3.9 ng/mL under the conditions of 0.75 μL Au-mAb and 450 nmol/L QDs-OVA, a bright green fluorescence signal was observed. As the SBT concentration increases to 250 ng/mL, the fluorescence signal on the T line is fully turned on, and the colorimetric signal is turned off. By comparison, Figure 5C shows that when the concentration of SBT reaches 15.6 ng/mL in the 2 μL of Au-mAb and 600 nmol/L QDs-OVA solutions, the fluorescence signal turns on. Therefore, 0.75 μL of Au-mAb and 450 nmol/L QDs-OVA were selected as the optimal experimental conditions.

Under the previous optimal experimental protocol, the sensitivity of the developed FICA was evaluated by a series of concentrations of SBT (0, 0.98, 1.95, 3.9, 7.8, 15.6, 31.25, 62.5, 125, and 250 ng/mL) in PBS (0.01 M, pH 7.4). Based on the changes in SBT concentration and T-line fluorescence intensity, a quantitative analysis curve was established, as shown in Figure 5D. The regression equation is $y = 11.2x + 134.8$ ($R^2 = 0.9829$), and the linear range is 3.9−62.5 ng/mL, LOD (defined as the T-line fluorescence intensity of the negative sample plus the lowest SBT concentration of 3 times the standard deviation) was 1.128 ng/mL, and when the concentration of SBT was 3.9 ng/mL, an obvious fluorescence signal was observed. Therefore, the vLOD was set to 3.9 ng/mL.

For comparison, previous reports for the determination of the SBT are summarized in Table 1. Among these methods, electrochemical sensors and SERS display extremely high sensitivity and can provide quantitative data. But these methods require relatively complicated operations, such as the process of adsorptive stripping pulse differential voltammetry (AdSDPV), preparation of the SERS substrate, and requirement of a device to record. By contrast, the FICA developed in this study exhibited a better LOD with other existing qualitative detection systems and even with other quantitative analysis procedures.

**Table 1. Overview of Recently Reported Methods for the Detection of SBT**

| method | qualitative/quantitative | lowest LOD | references |
|---|---|---|---|
| LFIA based on gold nanoparticle | qualitative | 500 ng/mL | 18 |
| FICA based on visual up conversion nanoparticle | qualitative | 20 ng/mL | 17 |
| colorimetric detection based on aggregation of AuNPs | quantitative | 1.15 μmol/L | 42 |
| paper device for distance-based | quantitative | 0.22 mmol/L | 1 |
| SERS | quantitative | $10^{-9}$ mol/L | 7 |
| carbon screen-printed electrode | quantitative | 0.3 μmol/L | 14 |
| FICA based on "turn-on" mode | qualitative | 3.9 ng/mL | this work |

**Specificity of the FICA.** To investigate the specificity of the FICA, the bioactive metabolites of SBT, *N*-desmethylsibutramine ($M_1$) and *N*,*N*-bidesmethylsibutramine ($M_2$) were tested by the FICA strips. Besides, sildenafil (SDF) was also regarded as a potential interfering substance because of its unexpected addition to slimming supplements.[43] As shown in Figure S2, no fluorescence signal could be observed even when M2 and SDF standards were added at a concentration of 1 μg/mL. Cross reactivity has been observed for the detection of $M_1$ and SBT standards at 10 ng/mL. We further evaluated the FICA developed for the detection of M1. The concentration of M1 was detected to be the same as that of SBT, and a standard curve was established (Figure S3). The regression equation was $y = 11.8x + 160.8$ ($R^2 = 0.9449$), the LOD was 2.087 ng/mL, and the vLOD was 7.8 ng/mL.

**Method Validation.** All sample preparation and extraction were as described previously. To remove the matrix effects, the finial extract was diluted 2, 4, 8, and 16-fold with 0.01 M PBS. Without SBT, the interference of the matrix was analyzed by the FICA assay using the pretreated blank sample, and the least dilution multiple could be ascertained when the fluorescence on the T line was quenched completely. The results of Figure S4 showed that the samples (both of the matrixes, dietary fiber soft gel, and tablet) needed to be diluted 16-fold to eliminate the matrix effects. Then, the sensitivity was evaluated by analyzing the two matrixes spiked at the different concentrations of SBT (0, 2, 5, 100, and 250 ng/mg) in the actual samples. Established LC−MS/MS for the detection of SBT was used to verify the accuracy of the FICA, with three replicate analyses in triplicate (Figures S5, S6). The lowest spiked concentration of 5 ng/mg was detected in dietary fiber soft gels and tablets, respectively. Qualitatively, all results of FICA and LC−MS/MS methods were consistent, and the corresponding quantitative results are shown in Table 2, which demonstrated the developed FICA possessing acceptable reliability and potential for future practical application.



https://doi.org/10.1021/acsomega.3c09050
ACS Omega 2024, 9, 7075−7084

Table 2. Verification of the Spiked Slimming Supplements Using LC−MS/MS and the Developed FICA in This Study

| Sample | Spiked (ng/mg) | LC-MS/MS detected (ng/mg) | Recovery (%) | RSD (%) | FICA-judgement[a] |
|---|---|---|---|---|---|
| Dietary fiber soft gel | 0 | ND[b] | ND | ND | − − − − − − |
| | 2 | ND | ND | ND | − − − − − − |
| | 5 | 4.65 | 93 | 6.38 | − − − + + + |
| | 100 | 94.66 | 94.66 | 6.01 | − − − + + + |
| | 250 | 234.45 | 93.8 | 4.74 | + + + + + + |
| Tablet | 0 | ND | ND | ND | − − − − − − |
| | 2 | ND | ND | ND | − − − − − − |
| | 5 | 5.21 | 104.2 | 5.04 | − − − + + + |
| | 100 | 96.73 | 96.73 | 4.85 | − − − + + + |
| | 250 | 234.11 | 93.64 | 6.12 | + + + + + + |

[a]Visual assessment: "− (red)" represents the negative result under natural light, "+ (red)" represents the positive result under natural light, "+ (green)" represents the negative result under UV light, and "+ (green)" represents the positive result under UV light. [b]Not detected.

## CONCLUSIONS

In this work, based on the fluorescence quenching effect of AuNPs on QD-OVA, a dual-signal FICA combining "turn-on" and "turn-off" modes is proposed for ultrasensitive on-site detection of SBT. Under the optimal detection condition, the lowest visual LOD and LOQ of the developed FICA for SBT was 3.9 ng/mL, 5.0 ng/mg. Its sensitivity was much higher than that of the traditional LFIA based on the "turn-off" mode. The developed FICA detection system has the advantages of fast detection speed, low cost, and high sensitivity, and the obtained results can be semiquantitative to the naked eye, demonstrating the potential application for the determination of sibutramine in weight loss supplements. However, before its commercial application, it requires validation for the stability and reproducibility of large-scale synthesis. In summary, the developed FICA detection system is expected to be a method suitable for rapid on-site screening.

## ASSOCIATED CONTENT

### Supporting Information

The Supporting Information is available free of charge at https://pubs.acs.org/doi/10.1021/acsomega.3c09050.

Chemical structure and synthetic route of hapten-SBT; specificity analysis of FICA; chemical structure of SBT, SDF, M1, and M2; elimination of matrix effects; and detection of SBT in spiked samples (PDF)

## AUTHOR INFORMATION


### Corresponding Author

**Cunzheng Zhang** − *State Key Laboratory of Food Science and Technology, Nanchang University, Nanchang 330047, P. R. China; Jiangsu Key Laboratory for Food Quality and Safety-State Key Laboratory Cultivation Base of Ministry of Science and Technology, Institute of Food Safety and Nutrition, Jiangsu Academy of Agricultural Sciences, Nanjing 210014, P. R. China; College of Plant Protection, Nanjing Agricultural University, Nanjing 210095, P. R. China;* orcid.org/0000-0001-5702-7480; Phone: 86-25-84390401; Email: zhcz2003@hotmail.com; Fax: 86-25-84390401

### Authors

**Yun Gui** − *State Key Laboratory of Food Science and Technology, Nanchang University, Nanchang 330047, P. R. China; Jiangsu Key Laboratory for Food Quality and Safety-State Key Laboratory Cultivation Base of Ministry of Science and Technology, Institute of Food Safety and Nutrition, Jiangsu Academy of Agricultural Sciences, Nanjing 210014, P. R. China*

**Yun Zhao** − *Jiangsu Key Laboratory for Food Quality and Safety-State Key Laboratory Cultivation Base of Ministry of Science and Technology, Institute of Food Safety and Nutrition, Jiangsu Academy of Agricultural Sciences, Nanjing 210014, P. R. China; State Key Lab of Food Science and Technology, Jiangnan University, Wuxi 214122, P. R. China*

**Pengyan Liu** − *Jiangsu Key Laboratory for Food Quality and Safety-State Key Laboratory Cultivation Base of Ministry of Science and Technology, Institute of Food Safety and Nutrition, Jiangsu Academy of Agricultural Sciences, Nanjing 210014, P. R. China*

**Yulong Wang** − *Jiangsu Key Laboratory for Food Quality and Safety-State Key Laboratory Cultivation Base of Ministry of Science and Technology, Institute of Food Safety and Nutrition, Jiangsu Academy of Agricultural Sciences, Nanjing 210014, P. R. China*

**Xinxin Mao** − *Jiangsu Key Laboratory for Food Quality and Safety-State Key Laboratory Cultivation Base of Ministry of Science and Technology, Institute of Food Safety and Nutrition, Jiangsu Academy of Agricultural Sciences, Nanjing 210014, P. R. China; College of Plant Protection, Nanjing Agricultural University, Nanjing 210095, P. R. China*

**Chifang Peng** − *State Key Lab of Food Science and Technology, Jiangnan University, Wuxi 214122, P. R. China;* orcid.org/0000-0003-0589-0455

**Bruce D. Hammock** − *Department of Entomology and Nematology and UCD Comprehensive Cancer Center, University of California, Davis, California 95616, United States;* orcid.org/0000-0003-1408-8317

Complete contact information is available at: https://pubs.acs.org/10.1021/acsomega.3c09050


### Author Contributions

Y.G.: data curation, formal analysis, investigation, methodology, and writing-original draft. Y.Z.: data curation, formal analysis, investigation, and methodology. P.-Y.L.: data curation and formal analysis. Y.-L.W.: data curation and methodology. X.-X.M.: data curation and investigation. C.-F.P.: formal analysis. B.D.H.: writing-review and editing. C.-Z.Z.: conceptualization, project administration, funding acquisition, and writing-review and editing.

### Notes

The authors declare no competing financial interest.

## ACKNOWLEDGMENTS

This work was supported by National Natural Science Foundation of China (32072311) and international cooperation program of Jiangsu (BX2021011); partial support was provided by NIH-NIEHS (RIVER Award) R35 ES030443-01 and NIH-NINDS U54 NS127758 (Counter Act Program);

and The Development of High Specificity Antibody and Its Application in Food Safety (S202105).

## REFERENCES

(1) Karamahito, P.; Sitanurak, J.; Nacapricha, D.; Wilairat, P.; Chaisiwamongkhol, K.; Phonchai, A. Paper device for distance-based visual quantification of sibutramine adulteration in slimming products. *Microchem. J.* **2021**, *162*, 105784.
(2) Luque, C. A.; Rey, J. A. The discovery and status of sibutramine as an anti-obesity drug. *Eur. J. Pharmacol.* **2002**, *440* (2−3), 119−128.
(3) Chung, J. Y.; Jang, S. B.; Lee, Y. J.; Park, M. S.; Park, K. Effect of CYP2B6 genotype on the pharmacokinetics of sibutramine and active metabolites in healthy subjects. *J. Clin. Pharmacol.* **2011**, *51* (1), 53−59.
(4) Morikawa, Y.; Shibata, A.; Okumura, N.; Ikari, A.; Sasajima, Y.; Suenami, K.; Sato, K.; Takekoshi, Y.; El-Kabbani, O.; Matsunaga, T. Sibutramine provokes apoptosis of aortic endothelial cells through altered production of reactive oxygen and nitrogen species. *Toxicol. Appl. Pharmacol.* **2017**, *314*, 1−11.
(5) Williams, G. Withdrawal of sibutramine in Europe. *Br. Med. J.* **2010**, *340*, c824.
(6) Youssef, R. M.; Khamis, E. F.; Korany, M. A.; Mahgoub, H.; Kamal, M. F. Microspectrometric determination of sibutramine in an adulterated slimming formulation. *Anal. Methods* **2014**, *6* (10), 3395.
(7) Liu, Z.; Gao, Y.; Jin, L.; Jin, H.; Xu, N.; Yu, X.; Yu, S. Core-Shell Regeneration Magnetic Molecularly Imprinted Polymers-Based SERS for Sibutramine Rapid Detection. *ACS Sustain. Chem. Eng.* **2019**, *7* (9), 8168−8175.
(8) Zhang, L.; Feng, R.; He, R.; Liang, Q. Detection and Verification of Sibutramine Adulterated in Herbal Slimming Supplements Using Electrospray Ionization Mass Spectrometry. *Bull. Korean Chem. Soc.* **2018**, *39* (4), 504−511.
(9) Ariburnu, E.; Uludag, M. F.; Yalcinkaya, H.; Yesilada, E. Comparative determination of sibutramine as an adulterant in natural slimming products by HPLC and HPTLC densitometry. *J. Pharm. Biomed. Anal.* **2012**, *64*−*65*, 77−81.
(10) Lanzarotta, A.; Lorenz, L.; Voelker, S.; Falconer, T. M.; Batson, J. S. Forensic Drug Identification, Confirmation and Quantification Using Fully Integrated Gas Chromatography with Fourier Transform Infrared Detection and Mass Spectrometric Detection (GC-FT-IR-MS). *Appl. Spectrosc.* **2018**, *72*, 750−756.
(11) Cebi, N.; Yilmaz, M. T.; Sagdic, O. A rapid ATR-FTIR spectroscopic method for detection of sibutramine adulteration in tea and coffee based on hierarchical cluster and principal component analyses. *Food Chem.* **2017**, *229*, 517−526.
(12) Ouyang, L.; Jiang, Z.; Wang, N.; Zhu, L.; Tang, H. Rapid Surface Enhanced Raman Scattering (SERS) Detection of Sibutramine Hydrochloride in Pharmaceutical Capsules with a β-Cyclodextrin- Ag/Polyvivnyl Alcohol Hydrogel Substrate. *Sensors* **2017**, *17* (7), 1601.
(13) Teradal, N. L.; Narayan, P. S.; Jaladappagari, S. Electro-reduced graphene oxide film modified glassy carbon electrode as an electrochemical sensor for sibutramine. *Anal. Methods* **2013**, *5* (24), 7090.
(14) Lima, A. B.; dos Santos, W. T. P.; Compton, R. G. Simple and Sensitive Determination of Sibutramine in Slimming Tea Beverages Using a Carbon Screen-printed Electrode with Adsorptive Stripping Voltammetry. *Electroanalysis* **2019**, *31* (5), 975−980.
(15) Huang, X.; Aguilar, Z. P.; Xu, H.; Lai, W.; Xiong, Y. Membrane-based lateral flow immunochromatographic strip with nanoparticles as reporters for detection: A review. *Biosens. Bioelectron.* **2016**, *75*, 166−180.
(16) Wang, Y.; Xu, J.; Qiu, Y.; Li, P.; Liu, B.; Yang, L.; Barnych, B.; Hammock, B. D.; Zhang, C. Highly Specific Monoclonal Antibody and Sensitive Quantum Dot Beads-Based Fluorescence Immunochromatographic Test Strip for Tebuconazole Assay in Agricultural Products. *J. Agric. Food Chem.* **2019**, *67* (32), 9096−9103.
(17) Zhang, S. W.; Sun, Y. Y.; Sun, Y. M.; Wang, H.; Li, Z. F.; Xu, Z. L. Visual upconversion nanoparticle-based immunochromatographic assay for the semi-quantitative detection of sibutramine. *Anal. Bioanal. Chem.* **2020**, *412* (29), 8135−8144.
(18) Suryoprabowo, S.; Liu, L.; Kuang, H.; Cui, G.; Xu, C. Gold immunochromatographic assay for simultaneous detection of sibutramine and sildenafil in slimming tea and coffee. *Sci. China Mater.* **2020**, *63* (4), 654−659.
(19) Gong, X.; Cai, J.; Zhang, B.; Zhao, Q.; Piao, J.; Peng, W.; Gao, W.; Zhou, D.; Zhao, M.; Chang, J. A review of fluorescent signal-based lateral flow immunochromatographic strips. *J. Mater. Chem. B* **2017**, *5* (26), 5079−5091.
(20) Grabolle, M.; Spieles, M.; Lesnyak, V.; Gaponik, N.; Eychmüller, A.; Resch-Genger, U. Determination of the Fluorescence Quantum Yield of Quantum Dots: Suitable Procedures and Achievable Uncertainties. *Anal. Chem.* **2009**, *81* (15), 6285−6294.
(21) Sun, Q.; Zhu, Z.; Deng, Q.-m.; Liu, J.-m.; Shi, G.-q. A "green" method to detect aflatoxin B1residue in plant oil based on a colloidal gold immunochromatographic assay. *Anal. Methods* **2016**, *8* (3), 564−569.
(22) López_Marzo, A. M.; Pons, J.; Blake, D. A.; Merkoci, A. High sensitive gold-nanoparticle based lateral flow Immunodevice for Cd2+ detection in drinking waters. *Biosens. Bioelectron.* **2013**, *47*, 190−198.
(23) Fu, Q.; Liang, J.; Lan, C.; Zhou, K.; Shi, C.; Tang, Y. Development of a novel dual-functional lateral-flow sensor for on-site detection of small molecule analytes. *Sens. Actuators, B* **2014**, *203*, 683−689.
(24) Bagdeli, S.; Rezayan, A. H.; Taheri, R. A.; Kamali, M.; Hosseini, M. FRET- based immunoassay using CdTe and AuNPs for the detection of OmpW antigen of Vibrio cholerae. *J. Lumin.* **2017**, *192*, 932−939.
(25) Esteve-Turrillas, F. A.; Abad-Fuentes, A. Applications of quantum dots as probes in immunosensing of small-sized analytes. *Biosens. Bioelectron.* **2013**, *41*, 12−29.
(26) Tan, X.; Li, Q.; Yang, J. CdTe QDs based fluorescent sensor for the determination of gallic acid in tea. *Spectrochim. Acta, Part A* **2020**, *224*, 117356.
(27) Sheng, W.; Chang, Q.; Shi, Y.; Duan, W.; Zhang, Y.; Wang, S. Visual and fluorometric lateral flow immunoassay combined with a dual-functional test mode for rapid determination of tetracycline antibiotics. *Microchim. Acta* **2018**, *185* (9), 404.
(28) Chen, M.; Li, H.; Shi, Z.; Peng, W.; Qin, Y.; Luo, R.; Zhou, D.; Gong, X.; Chang, J. High fluorescence quenching probe-based reverse fluorescence enhancement LFTS coupling with IS-primer amplification reaction for the rapid and sensitive Parkinson Disease-associated MicroRNA detection. *Biosens. Bioelectron.* **2020**, *165*, 112278.
(29) Hu, G.; Sheng, W.; Li, S.; Zhang, Y.; Wang, J.; Wang, S. Quantum dot based multiplex fluorescence quenching immune chromatographic strips for the simultaneous determination of sulfonamide and fluoroquinolone residues in chicken samples. *RSC Adv.* **2017**, *7* (49), 31123−31128.
(30) Hu, G.; Sheng, W.; Li, J.; Zhang, Y.; Wang, J.; Wang, S. Fluorescent quenching immune chromatographic strips with quantum dots and upconversion nanoparticles as fluorescent donors for visual detection of sulfaquinoxaline in foods of animal origin. *Anal. Chim. Acta* **2017**, *982*, 185−192.
(31) Fu, J.; Zhou, Y.; Huang, X.; Zhang, W.; Wu, Y.; Fang, H.; Zhang, C.; Xiong, Y. Dramatically Enhanced Immunochromatographic Assay Using Cascade Signal Amplification for Ultrasensitive Detection of Escherichia coli O157:H7 in Milk. *J. Agric. Food Chem.* **2020**, *68* (4), 1118−1125.
(32) Zhao, Y.; Huang, S.; Chao, M.; Wang, Y.; Liu, P.; Li, P.; Fang, X.; Routledge, M. N.; Peng, C.; Zhang, C. Highly resistant and sensitive colorimetric immunochromatographic assay for sibutramine (SBT) illegally adulterated into diet food based on PDA/AuNP labelling. *Analyst* **2023**, *148* (20), 5094−5104.
(33) Huang, X.; Ren, J. Gold nanoparticles based chemiluminescent resonance energy transfer for immunoassay of alpha fetoprotein cancer marker. *Anal. Chim. Acta* **2011**, *686* (1−2), 115−120.
(34) Yao, Y.; Guo, W.; Zhang, J.; Wu, Y.; Fu, W.; Liu, T.; Wu, X.; Wang, H.; Gong, X.; Liang, X. J.; Chang, J. Reverse Fluorescence


https://doi.org/10.1021/acsomega.3c09050
*ACS Omega* 2024, 9, 7075−7084

Enhancement and Colorimetric Bimodal Signal Readout Immunochromatography Test Strip for Ultrasensitive Large-Scale Screening and Postoperative Monitoring. *ACS Appl. Mater. Interfaces* **2016**, *8* (35), 22963−22970.
(35) Kholmicheva, N.; Razgoniaeva, N.; Yadav, P.; Lahey, A.; Erickson, C.; Moroz, P.; Gamelin, D.; Zamkov, M. Enhanced Emission of Nanocrystal Solids Featuring Slowly Diffusive Excitons. *J. Phys. Chem. C* **2017**, *121* (3), 1477−1487.
(36) Sekar, A.; Yadav, R.; Basavaraj, N. Fluorescence quenching mechanism and the application of green carbon nanodots in the detection of heavy metal ions: a review. *New J. Chem.* **2021**, *45* (5), 2326−2360.
(37) Zu, F.; Yan, F.; Bai, Z.; Xu, J.; Wang, Y.; Huang, Y.; Zhou, X. The quenching of the fluorescence of carbon dots: A review on mechanisms and applications. *Microchim. Acta* **2017**, *184* (7), 1899−1914.
(38) Nebu, J.; Anjali Devi, J. S.; Aparna, R. S.; Aswathy, B.; Lekha, G. M.; Sony, G. Fluorescence turn-on detection of fenitrothion using gold nanoparticle quenched fluorescein and its separation using superparamagnetic iron oxide nanoparticle. *Sens. Actuators, B* **2018**, *277*, 271−280.
(39) Chhabra, R.; Sharma, J.; Wang, H.; Zou, S.; Lin, S.; Yan, H.; Lindsay, S.; Liu, Y. Distance-dependent interactions between gold nanoparticles and fluorescent molecules with DNA as tunable spacers. *Nanotechnology* **2009**, *20* (48), 485201.
(40) Anfossi, L.; Di Nardo, F.; Cavalera, S.; Giovannoli, C.; Spano, G.; Speranskaya, E. S.; Goryacheva, I. Y.; Baggiani, C. A lateral flow immunoassay for straightforward determination of fumonisin mycotoxins based on the quenching of the fluorescence of CdSe/ZnS quantum dots by gold and silver nanoparticles. *Mikrochim. Acta* **2018**, *185* (2), 94.
(41) Larsson, T.; Wedborg, M.; Turner, D. Correction of inner-filter effect in fluorescence excitation-emission matrix spectrometry using Raman scatter. *Anal. Chim. Acta* **2007**, *583* (2), 357−363.
(42) Chaisiwamongkhol, K.; Labaidae, S.; Pon-in, S.; Pinsrithong, S.; Bunchuay, T.; Phonchai, A. Smartphone-based colorimetric detection using gold nanoparticles of sibutramine in suspected food supplement products. *Microchem. J.* **2020**, *158*, 105273.
(43) Hachem, R.; Assemat, G.; Martins, N.; Balayssac, S.; Gilard, V.; Martino, R.; Malet-Martino, M. Proton NMR for detection, identification and quantification of adulterants in 160 herbal food supplements marketed for weight loss. *J. Pharm. Biomed. Anal.* **2016**, *124*, 34−47.


https://doi.org/10.1021/acsomega.3c09050
*ACS Omega* 2024, 9, 7075−7084